

# Kinetic Modelling of Electrochemical Decolorization of Diazo Dyes on Boron-Doped Diamond Electrodes

Antonio Zuorro, Elisabetta Petrucci\*, Luca Di Palma, Roberto Lavecchia

Dipartimento di Ingegneria Chimica, Materiali e Ambiente, Sapienza Università di Roma, Via Eudossiana 18, 00184 Roma, Italy,  
\*elisabetta.petrucci@uniroma1.it

The anodic oxidation of diazo dyes on boron-doped diamond (BDD) electrodes in the presence of chloride was investigated. Reactive Green 19 (RG19), a relatively new diazo dye of high structural complexity, was used as a model dye. To evaluate the effect of the operating parameters on decolorization, electrolyses under galvanostatic conditions were performed in a membrane-free reactor. The results obtained suggest the simultaneous occurrence of a reaction mediated by hydroxyl radicals and a reaction mediated by active chlorine. The first reaction was found to be favored by increasing current density and temperature, while the second was promoted by acidic pH and by increasing chloride concentration and stirring rate. Several kinetic models were tested for their ability to correlate the experimental data. The best results were obtained by a power-law model including all the parameters of interest and using the time required to achieve 50% or 99% color removal as response variables. From the estimated model coefficients, the contribution of each operating parameter to RG19 decolorization at shorter and longer times was determined.

## 1. Introduction

Reactive diazo dyes are a class of compounds extensively used in the textile industry for their bright colors and resistance to fading. During the dyeing process, a competition occurs between the fixing reaction and the hydrolysis of the reactive group in the dye molecule, which results in a significant release of unfixed dye in the wastewater (Lewis et al., 2000). Due to the huge volume of effluents produced and the strong coloration imparted by even negligible amounts of dye, the environmental impact of textile wastewaters represents an issue of major concern (Caselatto et al., 2011). In fact, in addition to the toxicity and potential cancerogenicity of azo dyes, their presence in water bodies can reduce sunlight penetration and dissolved oxygen concentration, with deleterious effects on local flora and fauna.

For the above reasons, efforts are currently being devoted to finding practical and efficient solutions for the treatment of dye-containing wastewaters. In the field of advanced oxidation processes, the anodic oxidation on highly performant electrode materials, such as the boron-doped diamond (BDD) electrode, is attracting a great deal of attention. This anode presents unique characteristics in terms of electrochemical stability and resistance to chemical degradation. Moreover, its high overpotential for oxygen evolution allows the electrogeneration of large amounts of hydroxyl radicals that are slightly adsorbed on the electrode surface. Among the numerous applications of BDD electrodes, water disinfection (Petrucci et al., 2013), the removal and mineralisation of organic (Scialdone et al., 2008; Oturan et al., 2012) and inorganic (Montanaro et al., 2008) pollutants in aqueous solution and the treatment of real wastewaters (Tsantaki et al., 2012) have been the object of recent investigations.

In the anodic oxidation of dyes on BDD electrodes, the presence of chlorides, even at very low concentrations, can significantly enhance the decolorization rate, due to the high selectivity of the electrogenerated active chlorine for the chromophore groups (Montanaro and Petrucci, 2009). In the presence of chlorides, the reaction mediated by the electrogenerated active chlorine and that mediated by the hydroxyl radicals produced on BDD surface by water discharge occur simultaneously, leading to dye

decolorization and degradation. However, little attention has so far been devoted to evaluating the influence of individual process parameters upon the two reactions.

The main aim of the present work was to assess the contribution of the most important operating parameters, that is, dye and chloride concentrations, current density, pH, temperature and stirring rate, to the anodic oxidation of azo dyes on BDD electrodes. To this end, the sulfonated diazo dye Reactive Green 19 (RG19) was used as a model compound. The complex chemical structure of RG19, a high-molecular weight ( $M_w = 1418.9 \text{ g mol}^{-1}$ ) dye with two azo groups and two reactive chlorotriazine groups in its molecule, makes it an ideal candidate for this type of studies. Furthermore, attempts to degrade this dye by microbial (Saratale et al., 2009), photocatalytic (Rastegar et al., 2012) or UV/ $\text{H}_2\text{O}_2$  (Zuorro et al., 2013a) as well as the use of adsorbents (Zuorro et al., 2013b) have met only limited success.

To investigate the electrochemical oxidation kinetics of RG19 on BDD electrodes, the time required to achieve 50% or 99% decolorization was determined under different process conditions. Decolorization data were modelled by a power-law model and statistically analysed in order to evaluate the contribution of each parameter to the decolorization process.

## 2. Experimental

### 2.1 Materials

Unless otherwise indicated, sample solutions were prepared by dissolving in distilled water the appropriate amount of RG19 of technical grade ( $\text{C}_{40}\text{H}_{23}\text{Cl}_2\text{N}_{15}\text{Na}_6\text{O}_{19}\text{S}_6$ , color index number 205075, from Gammacolor Srl), 0.05 M  $\text{Na}_2\text{SO}_4$  and 0.01 M NaCl. Adjustments of pH were made using 96%  $\text{H}_2\text{SO}_4$  and 0.1 M NaOH. Reagents were supplied by Carlo Erba (Milano, Italy) and Sigma Aldrich (St. Louis, MO, USA) and were used without any further purification.

### 2.2 Electrochemical degradation experiments

The electrolytic cell was a cylindrical undivided reactor. The anode was a BDD electrode with a rectangular surface of  $5 \text{ cm}^2$  (Adamant Technologies) while the cathode was a commercial platinum wire (AMEL). They were placed in parallel at 1 cm of distance. 100 mL of dye solution were treated in each run. During the electrochemical treatment, the cell was thermostated and the electrolyte was magnetically stirred. The experiments were carried out under galvanostatic conditions using an AMEL 2051 potentiostat.

### 2.3 Analytical methods

The solution pH and conductivity were measured using a Crison GLP 421 and a Hanna Instrument HI87314. Absorbance was measured using a UV/Vis spectrophotometer (T80+ PG Instruments Ltd., Leicester, UK). RG19 decolorization was monitored by withdrawing about 3 mL of liquid samples at selected time intervals and calculating the degree of color removal (R%) as:

$$R\% = 100 \cdot \frac{A_0 - A_t}{A_0} \quad (1)$$

where  $A_0$  and  $A_t$  are the absorbance values, at time 0 and  $t$ , of the dye solution at 630 nm, where the absorption spectrum of the dye displays a sharp peak (Zuorro and Lavecchia, 2014). After analysis, the sample was immediately returned into the reactor.

Regression and statistical analysis was performed using Minitab® version 16.2.3 (State College, PA).

## 3. Results and discussion

### 3.1 Effect of operating parameters on dye decolorization

A large number of tests were performed to evaluate the effect of the main operating parameters on the degradation efficiency. In these experiments, chloride concentration was varied between 0 and 0.05 M, current density between 100 and 500  $\text{A m}^{-2}$ , pH between 3 and 11, temperature between 10 and 45 °C and stirring rate between 250 and 750 rpm. All runs were carried out in aqueous solutions containing 0.05 M sodium sulfate and a concentration of RG19 ranging from 50 to 150  $\text{mg L}^{-1}$ . Some representative results are shown in Figure 1.

From the results obtained, it can be seen that the addition of chloride greatly enhanced the decolorization of RG19, which can be ascribed to the synergistic effect of the indirect oxidation mediated by the electrogenerated active chlorine. In the presence of sodium chloride, decolorization was almost complete within the first 15 min of treatment, while in its absence a residual dye concentration was still found after six hours of electrolysis (data not shown). As expected, increasing current density was also beneficial, this effect being a result of the increased production of hydroxyl radicals and active chlorine. In particular, the

time of decolorization was approximately halved (from 23 to 11 min) as the current density was raised from 300 to 500 A m<sup>-2</sup>. The use of more acidic conditions resulted in a dramatic improvement in the reaction efficiency, the color removal reaching about 90%. Afterwards, the reaction rate underwent an abrupt decrease and complete decolorization was achieved in times comparable with those observed at higher pH. This trend was also observed at pH 4 and 5 (data not shown), confirming that two different reactions prevail at different treatment time intervals. Since pH strongly influences the equilibrium distribution of active chlorine species, favoring hypochlorous acid, which is an oxidizing agent stronger than hypochlorite, while <sup>•</sup>OH radicals are rather insensitive to this parameter, the results obtained suggest that the reaction mediated by active chlorine prevails at the initial stage of dye degradation. In contrast, the reaction mediated by hydroxyl radicals becomes prevalent only when most of the dye molecules have been degraded. We also note that a decrease in the stirring rate, after an initial negative effect, leads to complete decolorization with a slight time delay. This behavior can be explained by considering that, under the conditions employed, the active chlorine concentration becomes limiting and the attack to the chromophore, occurring in the initial stage, is favored by stirring. This effect seems to diminish when the prevailing reaction is that mediated by hydroxyl radicals.

### 3.2 Kinetic modeling of decolorization

A preliminary analysis of the experimental data showed that the decolorization process cannot be described by most common reaction rate expressions, such as the first-order or the zero-order kinetics, thus corroborating the hypothesis that different reactions take place simultaneously.

In consideration of the fact that the previously mentioned reactions prevail at different treatment times, the time intervals required to achieve 50% ( $\tau_{50}$ ) and 99% ( $\tau_{99}$ ) decolorization were determined from the experimental curves (see Figure 1). Different empirical models were then used to describe the dependence of  $\tau_{50}$  or  $\tau_{99}$  on dye and chloride concentrations, current density (J), temperature (T), pH and stirring rate (u). The best results were obtained by the following power-law expressions:

$$y = \prod_{i=1}^6 x_i^{a_i} \quad (2)$$

$$y = a_0 \prod_{i=1}^6 x_i^{a_i} \quad (3)$$

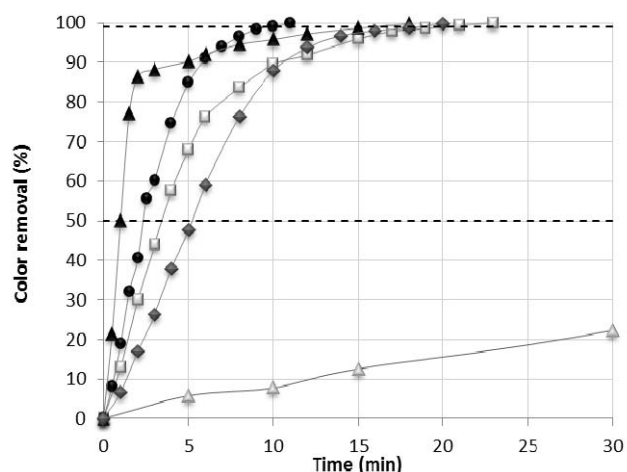


Figure 1: Color removal of solutions containing 100 mg L<sup>-1</sup> RG19, 0.05 M Na<sub>2</sub>SO<sub>4</sub>, T = 22 °C in electrolyses conducted in various conditions: pH = 5, J = 300 Am<sup>-2</sup>, NaCl = 0.01 M, u = 750 rpm (black triangle); pH = 7, J = 500 Am<sup>-2</sup>, NaCl = 0.01 M, 750 rpm (black circle); pH = 7, J = 300 Am<sup>-2</sup>, NaCl = 0.01 M, u = 750 rpm (white square); pH = 7, J = 300 Am<sup>-2</sup>, NaCl = 0.01 M, 250 rpm (black rhombus); pH = 7, J = 300 Am<sup>-2</sup>, NaCl = 0 M, 750 rpm (white triangle)

In the above equations,  $y$  is the response variable ( $\tau_{50}$  or  $\tau_{99}$ ),  $x_i$  are the independent variables,  $a_i$  are the coefficients associated to each independent variable and  $a_0$  is an empirical constant. For both responses, eq. (2) provided a more accurate fit and was therefore used to evaluate the six unknown parameters ( $a_i$ ). Parameter estimation was carried out by least-squares fitting of the data after linearization of eq. (2). Their values are listed in Table 1 together with their standard errors,  $t$  statistics and  $p$ -values. As apparent from the dispersion plot in Figure 2, the calculated values were in good agreement with the experimental results, and the points were uniformly distributed around the bisecting line. The resulting coefficient of determination ( $R^2$ ), adjusted- $R^2$  and prediction- $R^2$  were equal to 98.6%, 98.3% and 97.8%, for  $\tau_{50}$ , and 99.6%, 99.5% and 99.4%, for  $\tau_{99}$ , respectively. Analysis of residuals showed no apparent departures from basic ANOVA assumptions, i.e., normally distributed errors with constant variance and independent of one another (Figure 3).

Table 1: Regression coefficients of the power-law model (eq. 1) for the response variables  $\tau_{50}$  and  $\tau_{99}$ , with their standard errors (SE),  $t$ -statistics ( $t$ ) and  $p$ -values ( $p$ )

Time response	Coefficient	Associated variable	Value	SE	$t$	$p$
$\tau_{50}$	$a_1$	Dye concentration	0.504	0.057	8.898	<0.0001
	$a_2$	Chloride concentration	-0.772	0.050	-15.445	<0.0001
	$a_3$	Current density	-0.273	0.090	-3.016	0.005
	$a_4$	Temperature	-0.735	0.090	-8.222	<0.0001
	$a_5$	pH	0.345	0.106	3.257	0.003
	$a_6$	Stirring rate	-0.236	0.070	-3.394	0.002
$\tau_{99}$	$a_1$	Dye concentration	0.672	0.066	10.131	<0.0001
	$a_2$	Chloride concentration	-0.236	0.058	-4.032	<0.0001
	$a_3$	Current density	-0.341	0.106	-3.213	0.003
	$a_4$	Temperature	-0.769	0.105	-7.342	<0.0001
	$a_5$	pH	0.214	0.124	1.723	0.095
	$a_6$	Stirring rate	0.672	0.066	10.131	<0.0001

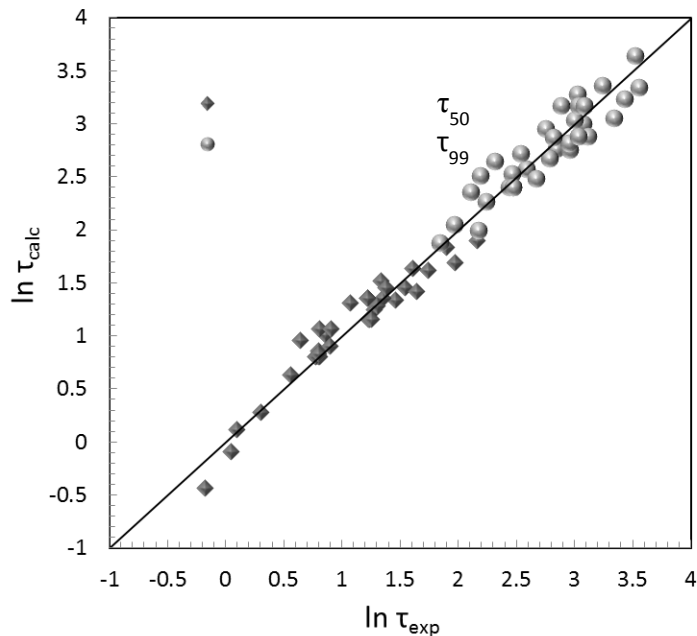


Figure 2: Comparison between experimental ( $\tau_{exp}$ ) and calculated ( $\tau_{calc}$ )  $\tau$ -values

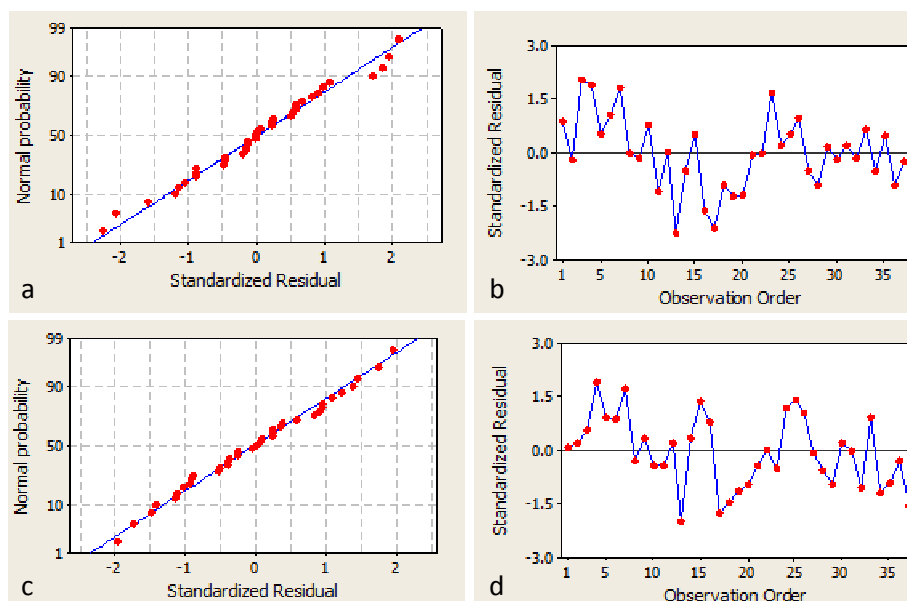


Figure 3: Normal probability plot and standardized residuals vs. observation order for  $\tau_{50}$  (a,b) and  $\tau_{99}$  (c,d)

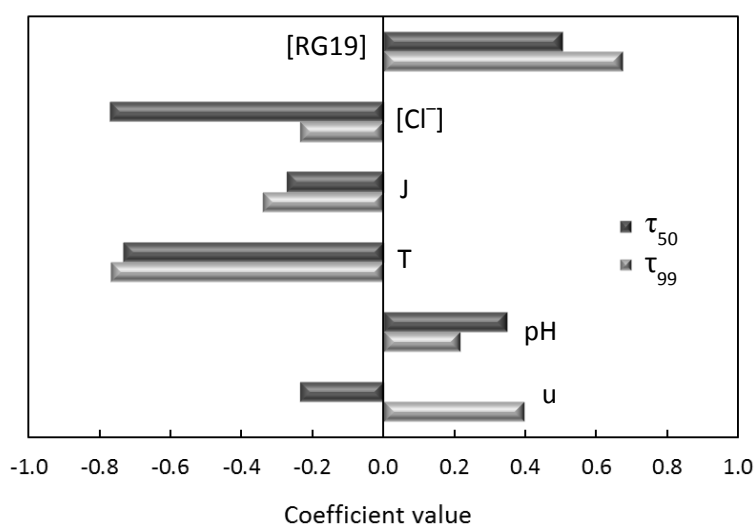


Figure 4: Estimated model coefficients showing the effect of each independent variable on  $\tau_{50}$  and  $\tau_{99}$

From Table 1, it can be seen that the estimated model coefficients were all statistically significant at the 99% confidence level ( $p < 0.01$ ), with the exception of the coefficient associated to pH, for  $\tau_{99}$ , which was significant at the 90% confidence level ( $p < 0.1$ ). It should be noted that the absolute value of each coefficient gives an indication of the contribution of the associated variable to the response variable. A positive coefficient indicates that the variable increases the  $\tau$ -value (i.e., negatively affects the decolorization kinetics), while the opposite holds for negative values of the coefficient.

Examination of Table 1 and Figure 4 reveals that the initial concentration of RG19, unlike other dyes investigated by the same workgroup (Montanaro and Petrucci, 2009), severely slows down the decolorization rate, especially when the reactions proceed to completion. A detrimental effect can also be observed for pH, which is more pronounced at lower times. In contrast, chloride addition had a positive effect on decolorization, which was more marked in the initial phase of the decolorization process. Also increases in temperature and current density were beneficial to decolorization, with comparable effects on

$\tau_{50}$  and  $\tau_{99}$ . As regards temperature, it should be noted that, although an increase in temperature promotes the evolution of gaseous chlorine, thus negatively affecting the concentration of active chlorine, it also improves the diffusion of the reacting species from the bulk of the solution to the electrode surface, and vice versa, with a net effect depending on the importance of each contribution.

The effect of agitation deserves particular attention. In fact, while at low conversions the stirring rate influenced positively the decolorization process, an opposite effect was observed at high conversions. A possible explanation is that at the initial stage of the process, when the reaction mediated by active chlorine is preponderant, agitation enhances the transport of reactants, positively affecting decolorization. However, as the reactions proceed, stirring of the solution can favor the formation of chlorates and perchlorates, thus reducing the availability of hydroxyl radicals for color removal (Aquino et al., 2013).

#### 4. Conclusions

The results of the present study indicate that the decolorization of RG19 on BDD electrodes proceeds through two distinct reactions, one mediated by active chlorine and the other by hydroxyl radicals. The kinetic model developed provides a simple and effective way to quantitatively evaluate the contribution of each process variable to the time intervals required to achieve 50% ( $\tau_{50}$ ) and 99% ( $\tau_{99}$ ) decolorization. The obtained results also suggest that the decolorization of azo dyes on BDD electrodes can be optimized by proper selection of process conditions. To this end, a statistical approach, such as the response surface methodology coupled with a factorial design including the most significant operating variables, could be effectively used.

#### References

- Aquino J.M., Rocha-Filho R.C., Rodrigo M.A., Sáez C., Cañizares P., 2013, Electrochemical degradation of the Reactive Red 141 dye using a boron-doped diamond anode. *Water Air Soil Poll.*, 224, 1397.
- Caselatto A.M.F., Ferrari Ferreira J., Basile Tambourgi E.B., Moraes R., Silveira E., 2011, Biodegradation of textile azo dyes by *Shewanella putrefaciens* (CCT 1967), *Chemical Engineering Transactions*, 24, 871–876.
- Lewis D.M., Renfrew A.H., Siddique A.A., 2000, The synthesis and application of a new reactive dye based on disulfide-bis-ethylsulfone, *Dyes Pigments*, 47, 151–167.
- Montanaro D., Petrucci E., 2009, Electrochemical treatment of Remazol Brilliant Blue on a boron-doped diamond electrode, *Chem. Eng. J.*, 153, 138–144.
- Montanaro D., Petrucci E., Merli C., 2008, Anodic, cathodic and combined treatments for the electrochemical oxidation of an effluent from the flame retardant industry, *J. Appl. Electrochem.*, 53, 947–954.
- Oturan, N., Brillas, E., Oturan, M.A., 2012, Unprecedented total mineralization of atrazine and cyanuric acid by anodic oxidation and electro-Fenton with a boron-doped diamond anode, *Environ. Chem. Lett.*, 10, 165–170.
- Petrucci E., Di Palma L., De Luca E., Massini G., 2013, Biocides electrogeneration for a zero-reagent on board disinfection of ballast water, *J. Appl. Electrochem.*, 43, 237–244.
- Rastegar M., Shadbad K.R., Khataee A.R., Pourrajab R., 2012, Optimization of photocatalytic degradation of sulphonated diazo dye C.I. Reactive Green 19 using ceramic-coated TiO<sub>2</sub> nanoparticles, *Environ. Technol.*, 33, 995–1003.
- Saratale R.G., Saratale G.D., Chang J.S., Govindwar S.P., 2009, Ecofriendly degradation of sulfonated diazo dye C.I. Reactive Green 19A using *Micrococcus glutamicus* NCIM-2168, *Biores. Technol.*, 110, 3897–3905.
- Scialdone O., Galia A., Guarisco C., Randazzo S., Filardo G., 2008, Electrochemical incineration of oxalic acid at boron doped diamond anodes: role of operative parameters. *Electrochim. Acta*, 53, 2095–2108.
- Tsantaki E., Velegraki T., Katsaounis A., Mantzavinos, D., 2012, Anodic oxidation of textile dyehouse effluents on boron-doped diamond electrode, *J. Hazard Mater.*, 207–208, 91–96.
- Zuorro A., Fidaleo M., Lavecchia R., 2013a, Response surface methodology (RSM) analysis of photodegradation of sulfonated diazo dye Reactive Green 19 by UV/H<sub>2</sub>O<sub>2</sub> process, *J. Environ. Manage.*, 127, 28–35.
- Zuorro A., Lavecchia R., 2014, Evaluation of UV/H<sub>2</sub>O<sub>2</sub> advanced oxidation process (AOP) for the degradation of diazo dye Reactive Green 19 in aqueous solution, *Desalin. Water Treat.*, 52, 1571–1577.
- Zuorro A., Lavecchia R., Medici F., Piga L., 2013b, Spent tea leaves as a potential low-cost adsorbent for the removal of azo dyes from wastewater, *Chemical Engineering Transactions*, 32, 19–24.